

# Cell culture density dependent toxicity and chromatin changes upon cadmium treatment in murine pre-B-cells

Gaspar Banfalvi · Kinga Ujvarosi · Gyorgy Trencsenyi · Csilla Somogyi · Gabor Nagy · Alexei Basnakian

Published online: 29 January 2007  
© Springer Science + Business Media, LLC 2007

**Abstract** Murine pre-B-cells grown in the presence of lower ( $1 \mu\text{M}$ ) or higher ( $5 \mu\text{M}$ ) concentration of cadmium chloride were separated into 13 fractions by centrifugal elutriation. The rate of DNA synthesis after cadmium treatment determined in permeable cells was dependent on cell culture density during cadmium treatment. Cell cycle analysis revealed a shift in the profile of DNA synthesis from replicative to repair DNA synthesis upon cadmium treatment. The study of the relationship between cell culture density and cell diameter at lower and higher cell densities in the presence of  $1 \mu\text{M}$  cadmium chloride concentration showed that a. at  $5 \times 10^5$  cell/ml or lower densities cells were shrinking indicating apoptotic changes, b. at higher cell culture densities the average cell size increased, c. the treatment of cells with low  $\text{CdCl}_2$  concentration ( $1 \mu\text{M}$ ) at higher cell culture density ( $> 5 \times 10^5$  cell/ml) did not change significantly the average cell diameter. At  $5 \mu\text{M}$  cadmium concentration and higher cell culture densities ( $> 5 \times 10^5$  cell/ml) the average cell size decreased in each elutriated fraction. Most significant inhibition of cell growth took place in early S phase (2.0–2.5 C value). Apoptotic chromatin changes in chromatin structure after cadmium treatment were seen as large extensive disruptions, holes in the nuclear membrane and stickiness of incompletely folded chromosomes.

**Keywords** Synchronization · Cell cycle · DNA synthesis · Reversible permeabilization · Interphase chromatin · Fluorescent microscopy · Apoptotic bodies

## Introduction

Cadmium is only weekly genotoxic, nevertheless it has been classified as carcinogen category 1 by the International Agency for Research on Cancer [1]. Cadmium is of worldwide concern because of its accumulation in the environment and long half-life estimated in humans to be between 15 and 20 years. Following long term exposure, the kidney is the critical organ [2]. Consequently a substantial amount of cadmium is accumulated in the organism over a number of years. Most important effects of high Cd-exposures are irreversible renal failure, immune deficiencies, bone disorders, obstructive airway disease [3].

At the cellular level, cadmium has multiple effects influencing differentiation, cell cycle progression, cell growth and it can induce apoptosis [4–8]. Cell death resulting from cadmium intoxication has been confirmed to occur through apoptosis by morphological and biochemical changes [9]. Cd caused morphological alterations in lung epithelial cells are characteristic of apoptosis, cell nucleus shrinkage is prominent, detachment of the cell from its neighbors, cytoplasmic and chromatin condensation, and fragmentation of the nucleus into multiple chromatin bodies surrounded by remnants of the nuclear envelope [10].

The induction of apoptotic cell death by cadmium was investigated in different mammalian cell lines and great differences in the cytotoxicity of cadmium were found, which could not be explained so far. Rat glioma C6 cells turned out to be sensitive with an  $\text{IC}_{50}$ -value of  $0.7 \mu\text{M}$ , while human adenocarcinoma A549 cells were relatively resistant

G. Banfalvi (✉) · K. Ujvarosi · G. Trencsenyi · C. Somogyi · G. Nagy  
Department of Microbial Biotechnology and Cell Biology,  
University of Debrecen, 1 Egyetem Square,  
Debrecen 4032, Hungary  
e-mail: bgaspar@delfin.klte.hu

A. Basnakian  
Division of Nephrology, University of Arkansas for Medical  
Sciences, Little Rock,  
AR 72205, USA

with an IC<sub>50</sub>-value of 164  $\mu\text{M}$  CdCl<sub>2</sub> [11]. The idea that glioma cell proliferation is controlled predominantly by cell size-dependent mechanisms [12] and the observation that adenocarcinoma is the most common form of non-small cell lung cancer [13] may be an indication that the occurrence of apoptosis after cadmium treatment may depend on cell size.

At molecular level cadmium affects DNA synthesis in a dose dependent manner. At concentrations higher than 1  $\mu\text{M}$  cadmium inhibits DNA synthesis [14], but very low cadmium concentrations stimulate DNA synthesis and cell proliferation [15]. Cadmium induces several genes involved in the stress response to pollutants or toxic agents. Several cell cycle regulating genes are over-expressed after exposure to cadmium, and many proteins are up-regulated such as proteins of the RAS signaling pathway and kinases of the RAS pathway. In conformity with the effects of cadmium at different concentrations we have found that by increasing the density in the CHO cell culture, a diminishing inhibitory effect on replicative DNA synthesis was measured. Flow cytometry revealed increasing cellular and nuclear sizes after 1  $\mu\text{M}$  CdCl<sub>2</sub> treatment in CHO cells [16] contradicting one of the most characteristic morphological changes of apoptosis known as cell shrinkage [11].

These conflicting observations raised several questions: 1. Is cadmium toxicity dependent on cell culture density, cell size or cell cycle stage? 2. What is the reason that low cadmium concentrations stimulate, higher cadmium concentrations inhibit DNA synthesis? 3. Why does Cd cause increase in cellular and nuclear size or result in morphological changes leading to cellular and nuclear shrinkage known as apoptosis?

Our recent results served as a basis to tackle these questions and led to the idea that Cd concentration might have been lowered by its binding to the cells [16]. The practical relevance of the confirmation of a stoichiometric relationship between toxicity and cell culture density could be the elimination or reduction of cadmium toxicity, by increasing the number of protective cells and/or metal binding proteins. In this paper we confirm the validity of the hypothesis regarding the stoichiometric relationship between cadmium toxicity and cell culture density. Differences in Cd toxicity were found during the cell cycle with higher cytotoxicity in early and late S, G2 and M phase than in mid S-phase. We confirm the shift from replicative to repair DNA synthesis and visualize apoptotic chromatin changes taking place after cadmium treatment during the cell cycle.

## Materials and methods

### Materials

The isotope [<sup>3</sup>H]-thymidine 5'-triphosphate (3.03 TBq mmole<sup>-1</sup>) was purchased from ICN Isotope and Nuclear.

Division (Irvine, CA, USA). 2,6-diamino-2-phenylindole (DAPI) was the product of Braunschweig Chemie (Braunschweig, Germany). Dextran T-150 was purchased from Pharmacia-Biochemicals (Gaitersburg, MD, USA). Colcemid (N-methyl-N-deacetyl-colchicine) was supplied by Boehringer (Mannheim, Germany). Growth media and sera were obtained from Invitrogen (Carlsbad, CA, USA). Nucleotides, 1,4-diazobicyclo-(2,2,2)-octane and other reagents were from Sigma-Aldrich Chemie GmbH (Munich, Germany).

Antifade Medium consisted of 90% glycerol, 2% (w/w) 1,4-diazobicyclo-(2,2,2)-octane, 20 mM Tris-Cl, pH 8.0, 0.02% sodium azide and 25 ng/ml DAPI for blue fluorescent total staining of DNA or of 0.2  $\mu\text{g/ml}$  propidium iodide for red DNA staining. Isotonic Buffer contained 140 mM sucrose, 60 mM KCl, 10 mM HEPES, pH 7.4, 5 mM KPO<sub>4</sub>, 5 mM MgCl<sub>2</sub>, 0.5 mM CaCl<sub>2</sub>. Hypotonic Buffer for reversible permeabilization contained 9 mM HEPES, pH 7.8, 5.8 mM dithiothreitol, 4.5% dextran T-150, 1 mM EGTA and 4.5 mM MgCl<sub>2</sub>. Swelling Buffer consisted of 50 mM KCl, 10 mM MgSO<sub>4</sub>, 3 mM dithiothreitol and 5 mM NaPO<sub>4</sub>, pH 8.0.

### Cell growth and cadmium treatment

The murine pre-B-cell line 70Z/3-M8 [17] was grown in suspension culture at 37°C in RPMI 1640 medium supplemented with 10% fetal calf serum, 2  $\mu\text{g/ml}$  mycophenolic acid, 150  $\mu\text{g/ml}$  xanthine, and 15  $\mu\text{g/ml}$  hypoxanthine and  $2 \times 10^{-5}$  M  $\beta$ -mercaptoethanol. Cells were grown for 9 h, and then treated with cadmium chloride (0.2–5  $\mu\text{M}$ ) at various cell densities ranging between  $10^5$ – $10^7$  cells/ml. Cells were grown for an additional 15 h in the presence of Cd before being harvested, unless otherwise noted. Before separation by elutriation cells were treated at 1 or 5  $\mu\text{M}$  concentration of CdCl<sub>2</sub>.

### Elutriation of cellular fractions

Based on the relationship between cell size and DNA content cells were separated by centrifugal elutriation and several fractions were collected. The cells within each fraction belonged to the same cell cycle phase, i.e. they were synchronous in each elutriation fraction. Fractionation was performed by counterflow centrifugal elutriation. Cells were grown for 15 h to a final concentration of  $2$ – $4 \times 10^5$  cells/ml, harvested by centrifugation at  $600 \times g$  for 5 min at 5°C, collected in 13 fractions and resuspended in RPMI 1640 medium containing 1% FBS at  $10^7$  cells/ml. Cells ( $2.2 \times 10^8$ ) were introduced into the elutriator rotor (Beckman J-6 MI) equipped with a JE-5.0 elutriation system including a Sanderson chamber (Beckman Instruments, Inc., Palo Alto, CA) and a MasterFlex peristaltic pump (Cole-Parmer

Instruments). Elutriation was performed at 20°C. Thirteen cell fractions (100 ml each) were collected by elution in RPMI medium containing 1% fetal bovine serum at increasing flow rates. The fraction collected during loading, which contained dead cells, was discarded. The first fraction, which contained primarily G<sub>1</sub> cells, was not used for the study of chromatin condensation. Each fraction was routinely monitored by light microscopy and analyzed by fluorescence activated cell sorting (FACS). The fractions contained unaggregated cells, which increased in size with each fraction elutriated. Cell number, size and volume were determined using a Coulter Multisizer (Beckman Coulter). Cell number was also assessed in a Burkner chamber and viability (> 98%) was determined by trypan blue dye exclusion in each fraction. All experiments were repeated three times with similar results.

#### FACS analysis of cell cycle

Cells were fixed with 70% methanol at room temperature and stained with 50 µg/ml propidium iodide (Sigma). The cells were analyzed by a FACScan flow cytometer (Becton Dickinson) using the CellQuest (Becton Dickinson) software as described [17]. The nuclear DNA content, expressed in C values (1C value corresponds to a haploid DNA content per cell) increased from 2C to 4C and provided a measure of progression through the S phase. Flow cytometric profiles giving the distribution of DNA content were used to calculate the average C-value for each elutriated fraction. The cells in each fraction were divided into 17 subfractions to cover the total area of the cytometric profile. C-values were calculated from the appropriate area under the flow cytometric profile and were averaged to yield the DNA content for each fraction as described previously [18].

#### Reversible permeabilization

This method, originally developed for the reversible permeabilization of murine lymphocytes [19] was adapted to murine pre-B-cells. Briefly, 1 ml of Hypotonic Buffer was added to 10<sup>6</sup> cells in the presence of Dextran T-150 as a molecular coat to prevent cells from disruption. Permeabilization was carried out for 2 min at 0°C. For reversal of permeabilization, the hypotonic solution was replaced by RPMI 1640 medium containing 10% fetal bovine serum, and the cells were incubated in a CO<sub>2</sub> incubator at 37°C and 5% CO<sub>2</sub> for 4 h.

#### ATP-dependent replicative DNA synthesis in permeable cells

Cells (0.2 or 1 × 10<sup>6</sup>) were permeabilized and replicative DNA synthesis was carried out as described [21].

The mixture (100 µl) contained 100 mM HEPES pH 7.8, 210 mM NaCl, 15 mM ATP, 0.3 mM dATP, dGTP, and dCTP, 0.01 mM dTTP, 37 kBq [<sup>3</sup>H]dTTP (3.03 TBq mmole<sup>-1</sup>), 5.8 mM dithiothreitol (DTT), 2 mM MgCl<sub>2</sub>, and 0.2 mM CaCl<sub>2</sub>. After 30 min of incubation at 37°C, the reactions for DNA synthesis were stopped by the addition of 1 ml 5% TCA. After standing in ice for 1 h, the precipitates were washed on glass fiber filters and counted for TCA insoluble radioactivity.

#### ATP-independent repair DNA synthesis in permeable cells

Cells (0.2 or 1 × 10<sup>6</sup>) were permeabilized and repair DNA synthesis was carried out as described [20]. The mixture (100 µl) contained 100 mM HEPES pH 7.8, 210 mM NaCl, 0.3 mM dATP, dGTP, and dCTP, 0.01 mM dTTP, 37 kBq [<sup>3</sup>H]dTTP (3.03 TBq mmole<sup>-1</sup>), 5.8 mM dithiothreitol (DTT), 2 mM MgCl<sub>2</sub>, 0.2 mM CaCl<sub>2</sub>, 1% glycerol and 0.4 units of *E. coli* glycerokinase. After 30 min of incubation at 37°C, the reactions for DNA synthesis were stopped by the addition of 1 ml 5% TCA. After standing at 0°C for 1 h, the precipitates were washed on glass fiber filters and counted for TCA insoluble radioactivity.

#### Isolation of nuclei

On account of the cyclic character of chromatin unfolding and chromosome condensation, which is limited to a relatively short time, synchronized cell populations were treated with colcemid to arrest the cycle in metaphase. Cells (10<sup>6</sup>) were resuspended in growth medium after reversal of permeabilization and treated with 0.1 µg/ml colcemid for 2 h at 37°C under 5% CO<sub>2</sub>. Cells were washed with PBS and incubated at 37°C for 10 min in Swelling Buffer, followed by centrifugation at 500 × g for 5 min. Nuclei were isolated by the slow addition of 20 volumes of Fixative (methanol:glacial acetic acid, 3:1) and were then centrifuged at 500 × g for 5 min, washed twice in Fixative and resuspended in 1 ml of Fixative. Cellular and nuclear volumes and nuclear diameter were determined with the Coulter Multisizer.

#### Spreads of nuclear structures

Preparation of nuclei for spreads of chromatin structures used the method developed for metaphase chromosomes. Nuclei were centrifuged at 500 × g for 5 min, washed twice in Fixative and resuspended in 1 ml Fixative. Nuclei were spread over glass slides dropwise from a height of approximately 30 cm. Slides were air dried, stored at room temperature overnight, rinsed with PBS and dehydrated using increasing concentrations of ethanol (70, 90, 95 and 100%).

## Visualization of chromatin structures

Dehydrated slides containing isolated chromatin structures were mounted in 35  $\mu$ l Antifade Medium under 24  $\times$  50 mm coverslips. Blue fluorescence of DAPI was monitored with an Olympus AX70 fluorescence microscope.

## Results

### Effect of cadmium on replicative DNA synthesis in permeable cells

When murine pre-B-cells were treated with 1  $\mu$ M CdCl<sub>2</sub> at three cell culture densities, more than 60% inhibition of replicative DNA synthesis was obtained at 10<sup>5</sup> cells/ml and a gradual decrease in nucleotide incorporation was observed between 1 and 24 h. When the same Cd treatment was applied at culture density of 2.5  $\times$  10<sup>5</sup> cells/ml, the initial lower level of DNA synthesis (> 50%) was maintained throughout the 24 h treatment. In cell cultures containing 5  $\times$  10<sup>5</sup> cell/ml, the initial inhibition ( $\approx$  40%) of DNA synthesis gradually decreased and reached the control level of DNA synthesis in 12 h. These results are similar to those observed in CHO cells [16] and indicate that intracellular Cd concentration is likely to be lowered by its binding to metallothionein and other proteins [21]. If this would be the case one would expect a significant difference between the toxic effects of lower and higher metal ion concentrations and apoptotic effects could be eliminated or at least reduced by increasing cell culture density. To test this possibility we have determined the cell culture density (10<sup>5</sup> cells/ml) and the corresponding cadmium concentration causing 50% inhibition in DNA replication. Gradual decrease in replicative DNA synthesis upon 0.2, 0.5, 1, 2 and 5  $\mu$ M CdCl<sub>2</sub> treatment was observed, causing 8, 21, 27, 39 and 51% inhibition, respectively (Fig. 1).

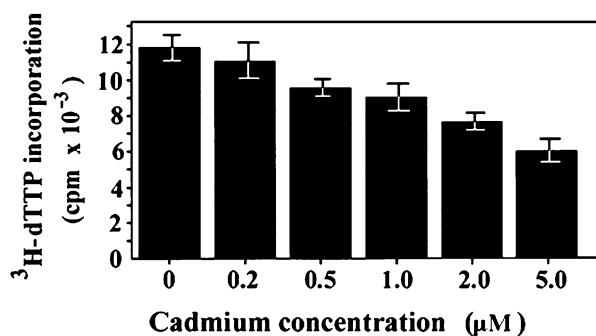


**Fig. 1** Inhibition of replicative DNA synthesis at different cadmium concentration. Cell growth of six cell cultures each started at 10<sup>5</sup> cell/ml each in the presence of 0.2, 0.5, 1, 2 and 5  $\mu$ M CdCl<sub>2</sub>, respectively. Cadmium treatment lasted for 15 h. After treatment 10<sup>6</sup> cells from each population were permeabilized and replicative DNA synthesis was measured. [<sup>3</sup>H]-thymidine triphosphate incorporation was measured as acid insoluble radioactivity as described in the Materials and Methods

### Effect of cadmium concentration on cell growth during the cell cycle

Two concentrations of cadmium (1 and 5  $\mu$ M) have been chosen to determine which stage of the cell cycle is most vulnerable to heavy metal treatment. Cell cultures were grown at an initial density of 1.2  $\times$  10<sup>5</sup> cells/ml in the absence and in the presence of 1 and 5  $\mu$ M CdCl<sub>2</sub>. Cell growth measured in a cell cycle dependent manner showed a significantly higher inhibitory effect of cadmium in mid-S phase (Fig. 2). Detailed analysis of cadmium inhibition on cell growth is summarized in Table 1. Treatment with 1 and 5  $\mu$ M CdCl<sub>2</sub> caused an overall 38 and 66% cell growth inhibition, respectively. Most significant reduction in cell number occurred in elutriation fraction 6, corresponding to mid S phase.

Elutriation fractions of control (untreated) and cadmium treated (1  $\mu$ M) cells (Fig. 2) were subjected to flow cytometric analysis (Fig. 3). These measurements revealed that C-values of untreated cells increased from 2C to 4C (Fig. 3(A)), while the C-values of cadmium treated cells were higher in each elutriated fraction (Fig. 3(B)). One would expect that the higher C-values reflect increased DNA content, coming from the elevated rate of DNA synthesis. Consequently we have measured replicative and repair DNA synthesis in elutriated fractions after Cd treatment to find an explanation to the increased fluorescence.

The fact that the smaller glioma cells were more sensitive to cadmium treatment than larger adenocarcinoma cells

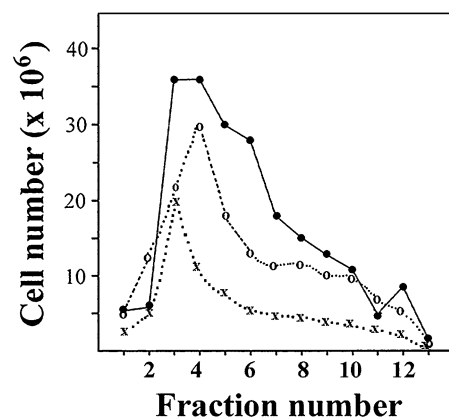


**Fig. 2** Elutriation profiles of exponentially growing cells before and after cadmium treatment. Three suspension cultures (1 liter each) of murine pre-B-cells (at 1.2  $\times$  10<sup>5</sup> cells/ml) were grown in spinner flasks for 15 h in RPMI medium supplemented with 10% fetal bovine serum. Control (untreated) cells were harvested at 2.2  $\times$  10<sup>5</sup> cells/ml by centrifugation at 600  $\times$  g for 5 min at 5°C and resuspended in 20 ml elutriation medium containing RPMI medium and 1% fetal bovine serum. Control cells (2.2  $\times$  10<sup>8</sup>) were loaded into a Beckman JE6B elutriator rotor and elutriation was carried out as described in the Methods (●-●). The same experiment was carried out with the exception that cells were grown to 1.7  $\times$  10<sup>5</sup> cell/ml in the presence of 1  $\mu$ M CdCl<sub>2</sub> and 1.7  $\times$  10<sup>8</sup> cells were loaded into the elutriation chamber (○-○). In the third experiment cells were grown in the presence of 5  $\mu$ M CdCl<sub>2</sub>, harvested at 8  $\times$  10<sup>4</sup> cells/ml and 8  $\times$  10<sup>7</sup> cells were subjected to elutriation (x-x-x)

**Table 1** Cadmium induced inhibition of cell growth during the cell cycle

Fraction number	Cell cycle phase	Elutriated					
		Control		1 $\mu\text{M}$ CdCl <sub>2</sub>		5 $\mu\text{M}$ dCl <sub>2</sub>	
		$\times 10^6$ cells	%	$\times 10^6$ cells	%	$\times 10^6$ cells	%
1	discarded	5.5	2.54	5.1	2.36	2.2	1.01
2	early S	6	2.78	12.5	5.78	5.2	2.41
3	early S	36	16.67	22	10.19	20.3	9.39
4	early mid S	36.5	16.90	30.3	14.02	11.8	5.46
5	early mid S	30	13.68	17.5	8.10	7.5	3.47
6	mid S	28	12.96	13.5	6.25	5.2	2.41
7	mid S	18	8.33	12	5.56	4.8	2.22
8	late mid S	16	7.41	12.5	5.78	4.8	2.22
9	late mid S	14	6.48	11	5.09	4.0	1.85
10	late S	12	5.56	10.5	4.86	3.8	1.76
11	late S, G2,M	5	2.31	7.5	3.47	2.4	1.11
12	late S, G2, M	8	3.70	6	2.78	2.0	0.93
13	late S, G2, M	1	0.46	0.5	0.23	0.2	0.09
Elutriated total:		216 $\times 10^6$	100%	160.9 $\times 10^6$	61.9%	74.2 $\times 10^6$	34.4%

Loaded control population ( $2.16 \times 10^8$ ) was taken as 100%.

Percentage of cell number in each fraction is expressed as % of the total population.

Control cells subjected to elutriation:  $2.2 \times 10^8$ .

Loss during manipulation:  $4 \times 10^6$  (1.8%).

Cadmium treated cells (1  $\mu\text{M}$ ) subjected to elutriation:  $1.7 \times 10^8$ .

Loss of Cd treated (1  $\mu\text{M}$ ) cells during manipulation:  $9.1 \times 10^6$  (5.4%).

Cadmium treated cells (5  $\mu\text{M}$ ) used for elutriation:  $8 \times 10^7$ .

Loss of Cd treated (5  $\mu\text{M}$ ) cells during manipulation:  $5.8 \times 10^6$  (7.3%).

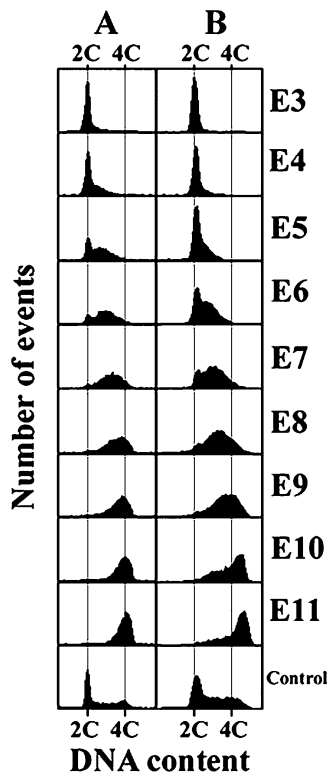


**Fig. 3** Flow cytometry of murine pre B cells before (A) and after (B) 1  $\mu\text{M}$  CdCl<sub>2</sub> treatment. The DNA content of each elutriation fraction is indicated as haploid genome content (C-value) on the abscissa and cell number is given on the ordinate. Controls are representing unelutriated cells before and after cadmium treatment

[11] raised the question whether or not the cytotoxic effect of cadmium toxicity depends on cell size within the same species. The cell size was measured in elutriated fractions following toxic treatment (5  $\mu\text{M}$  CdCl<sub>2</sub>). The relationship between cell cycle distribution versus cell diameter in control untreated and treated cells is shown in Fig. 4. The size of untreated cells is significantly higher in each elutriated fraction (Fig. 4(A), (C)) than the size of Cd treated and thus apoptotic cells (Fig. 4(B) and (C)). Smaller cells seem to be more vulnerable particularly in early S phase (Fig. 4(C), fractions 2, 3). However, the curve showing the limited increase in cell size during the cell cycle also indicates that cadmium has a more toxic effect in late S, G2 and M phase (Fig. 4(C), fractions 8–12) than in mid S phase (Fig. 4(C), fractions 4–6). Consequently a direct relationship between cell size and cadmium toxicity can be ruled out.

Replicative and repair DNA synthesis during the cell cycle

DNA synthesis in permeable cells was measured in elutriated fractions under replicative and repair synthesis conditions after cadmium (5  $\mu\text{M}$ ) treatment (Fig. 5). The simultaneous measurement of replicative and repair DNA synthesis showed a typical biphasic, but reduced replicative DNA profile (Fig. 5(A)), and an increased repair DNA synthesis throughout the cell cycle (Fig. 5(B)). The shift in the two peaks indicate that replicative and repair DNA synthesis are temporally distinct processes.



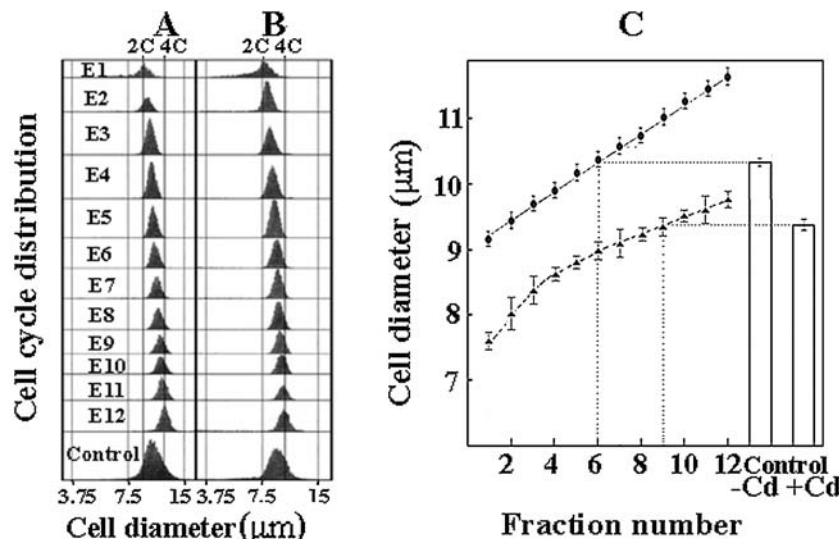


**Fig. 4** Cell cycle analysis of murine pre-B-cells before (A) and after 5  $\mu\text{M}$   $\text{CdCl}_2$  treatment (B). Cell cycle distribution on Coulter multisizer II is given on the ordinate and cell diameter on the abscissa. The DNA content of each elutriation fraction (E1-E12) is indicated by the haploid genome content (average C-value from 2C to 4C). The continuity of

the normal cell growth is disrupted by cadmium treatment in elutriation fractions (C). Cell growth in elutriated fractions in the absence ( $\bullet$ - $\bullet$ ) and in the presence ( $\blacktriangle$ - $\blacktriangle$ ) of 5  $\mu\text{M}$   $\text{CdCl}_2$ . Controls are representing unelutriated cells before and after cadmium treatment

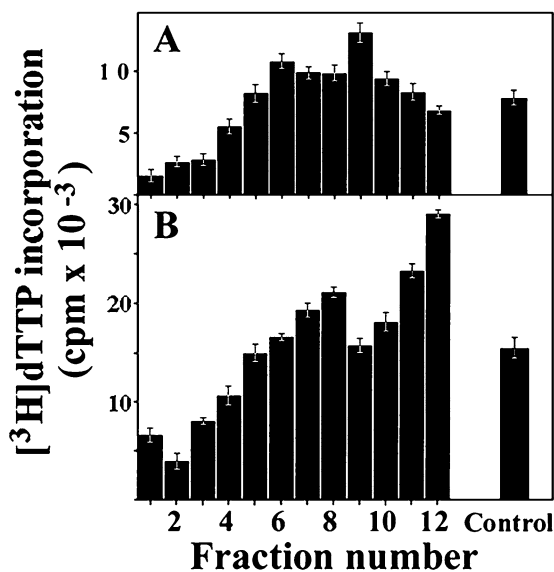


**Fig. 5** Replicative and repair DNA synthesis in permeable cells of elutriated fractions after cadmium treatment. [ $^3\text{H}$ ]-thymidine triphosphate incorporation was measured under replicative (A) and repair conditions (B) after cadmium chloride (5  $\mu\text{M}$ ) treatment. Elutriation, [ $^3\text{H}$ ]-dTTP incorporation and cadmium treatment were carried out as described in the Materials and Methods

In CHO cells cadmium induced oxidative damage reduced ATP-dependent nucleotide incorporation reflecting DNA replication but ATP-independent repair synthesis was elevated in certain subphases of the cell cycle [22].

#### Relationship between cell density and cadmium toxicity

To test the validity of a stoichiometric relationship between cell density and apoptosis, six cell cultures with different

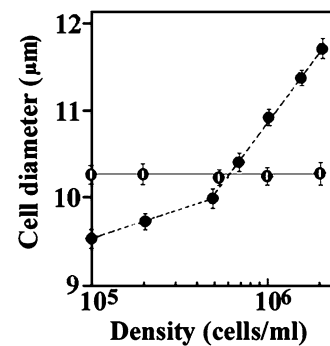


**Fig. 6** Cadmium induced changes in cell size at different cell densities. Logarithmic growth of cell cultures was allowed to continue at different cell densities ( $10^5$ ,  $2 \times 10^5$ ,  $5 \times 10^5$ ,  $10^6$ ,  $1.5 \times 10^6$  and  $2 \times 10^6$  cells/ml) in the presence and absence of 5  $\mu\text{M}$   $\text{CdCl}_2$ . Cell diameter was measured on Coulter Multisizer II

cell densities were grown in the presence of 5  $\mu\text{M}$   $\text{CdCl}_2$  and cell diameters were measured after 15 h of treatment. In Fig. 6 the shrinking of cells can be observed at cell densities  $\leq 5 \times 10^5$  cells/ml, while at higher than  $5 \times 10^5$  cells/ml the cell diameter was increasing.

#### Interphase chromatin structures in untreated cells

Interphase chromatin structures in murine pre-B-cells have been described earlier at lower resolution of centrifugal elutriation by collecting eight fractions [23]. When higher resolution was used (13 fractions) the same chromatin structures were visualized after DAPI staining (Fig. 7). These structures include veil-like nuclear material with some polarization of the chromatin in early S phase (Fig. 7(a)–(d)), fibrous structures in early mid S phase (Fig. 7(e)–(h)),

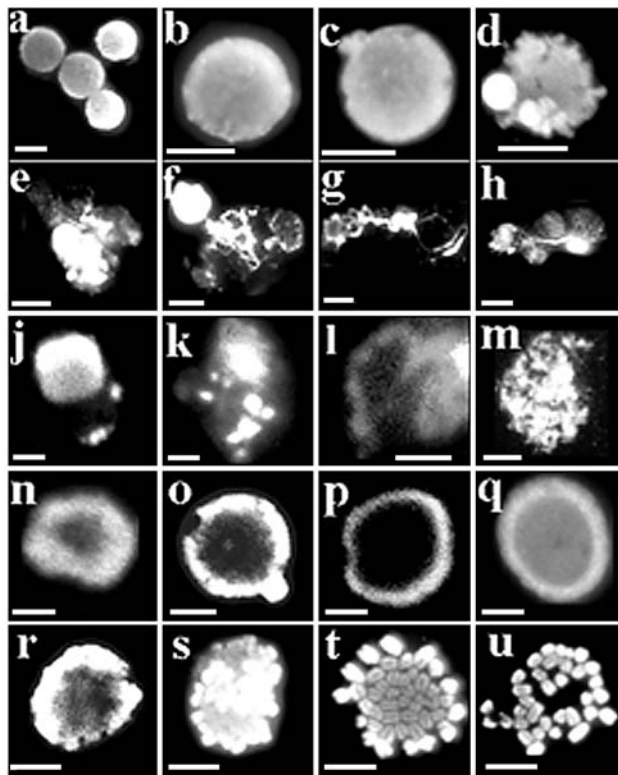


**Fig. 7** Intermediates of chromatin condensation in untreated pre-B-cells. Reversal of permeabilization of elutriated cells was followed by colcemid treatment and isolation of chromatin structures as described in the Methods. Regular structures after DAPI staining seen under fluorescence microscope: fractions 2–3, polarized nuclear material (a–d) fractions 4–6, extrusion of fibrillar chromatin (e–h) fractions 7–8, formation of chromatin bodies (j)–(m) fractions 9–10, ribboned chromatin (n)–(q); fractions 11–12, precondensed chromosomes (r)–(u). Bars 5  $\mu$ M each

chromatin bodies in mid S phase (Fig. 7(n)–(m)), chromatin ribbon later in mid S phase (Fig. 7(n)–(q)), precondensed chromosomes in late S, G2 and M phases (Fig. 7(r)–(u)). As exponentially growing cell cultures were used, the contribution of G2 and M phase cells (fractions 11–13) to the total cell population was only 6.5% (Table 1).

#### Apoptotic changes in chromatin structure after cadmium treatment

The cell size distribution after cadmium treatment already indicated the high vulnerability of cells in early S-phase. Fluorescent images of chromatin changes confirmed this notion by the appearance of apoptotic bodies in early S-phase (Fig. 8, Fraction 2) which is related to premature chromatin condensation. The polarization of the nuclear material and extrusion of the nuclear material of looped chromatin veil are typical structures later in early S phase (Fig. 8, fraction 3). Chromatin margination after cadmium treatment in early mid S phase and the absence of supercoiled loops were

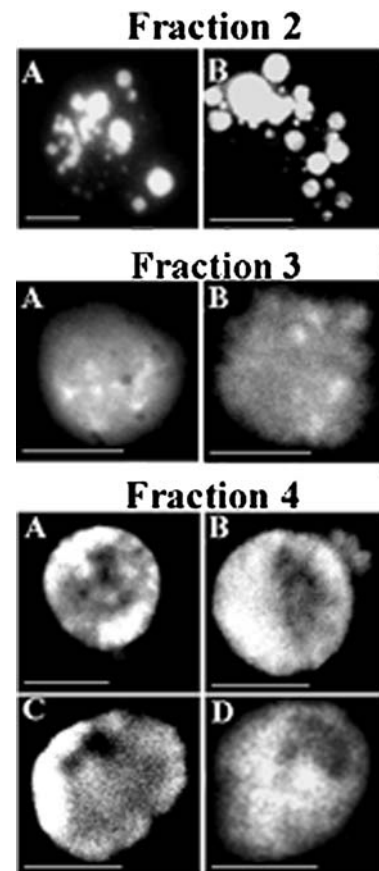


**Fig. 8** Cadmium induced chromatin changes in early S phase (Elutriation Fraction 2–4). Cells ( $2 \times 10^5$ /ml) were subjected to 1  $\mu$ M CdCl<sub>2</sub> treatment followed by reversible permeabilization and isolation of chromatin structures as described in the Methods. Fluorescent microscopy after DAPI staining was carried out. Bars 5  $\mu$ m each

found preventing the formation of chromatin bodies (Fig. 8, fraction 4).

Reversible permeabilization allowed to open the nucleus any time during the cell cycle in untreated cells. After cadmium treatment the increasing stickiness of the nuclear material prevented the opening of the nucleus and obscured the events of chromatin condensation. The formation of perinuclear granules (Fig. 9, fraction 6) and ribboned chromatin arranged in a semicircular manner is evident (Fig. 9, fraction 8).

Most typical changes of cadmium treatment are the severe disruptions of the nuclear membrane observed in fraction 10 (Fig. 10, fraction 10). These disruption did not allow to distinguish among the final stages of chromatin condensation, resulting in nuclei with big holes inside them and sticky imperfectly condensed chromosomes (Fig. 10, fraction 12).

#### Discussion

Our earlier observation that cadmium has an effect on the relationship between cell culture density and the rate of DNA

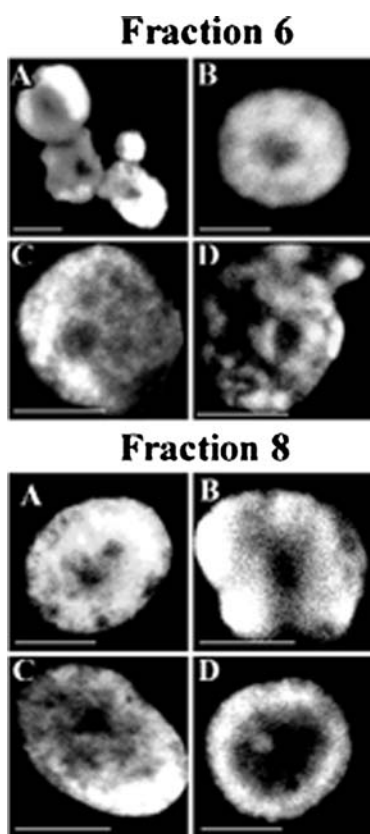


**Fig. 9** Cadmium induced chromatin changes in mid S phase (Elutriation Fraction 6–8). Cells were treated and chromatin structures were isolated as described under Fig. 7. Typical changes in elutriation fraction 6: disruptions (A, D) and holes in the nuclear membrane (B, C) and in elutriation fraction 8: large-sized perinuclear granules and holes in the middle of the nucleus (A)–(D). Bars 5  $\mu\text{m}$  each

replication suggested that cell growth and DNA synthesis at higher cell concentration could be suppressed by increasing Cd concentration. The connection between cell growth and cadmium concentration pointed to the stoichiometric binding of cadmium to CHO cells [16]. An extension of this idea was that the cytotoxicity of cadmium could be eliminated or at least minimized by increasing cell culture density. This observation raises the question whether only specific cadmium-binding (metallothionein) proteins are involved in the protective mechanism against the toxic cadmium ion, or non-specific binding may also be involved. Nephrotoxic studies after cadmium exposure indicate that pretreatment with cadmium effectively induced the metallothionein synthesis. Cadmium was mainly bound to metallothionein and other low molecular weight proteins in pretreated mammals, while in non-pretreated animals the major part of Cd was bound to high molecular weight proteins [21]. These experiments are in conformity with our experiments regarding the possibility of using inert proteins to lower cadmium toxicity.

The distribution of peaks of nuclear growth after cadmium treatment showed similarities to the number and position of

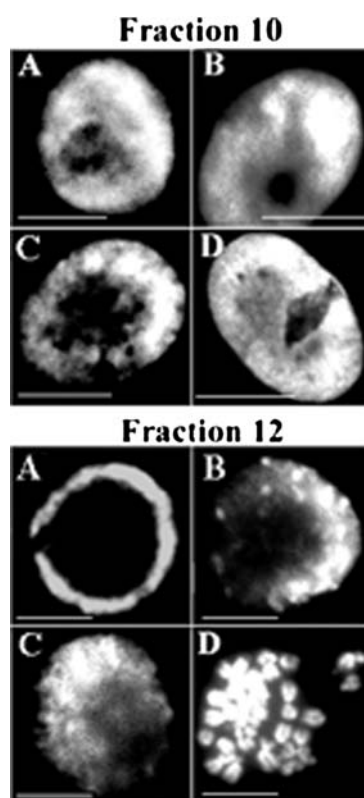


**Fig. 10** Cadmium induced chromatin changes at the end of S, G2 and in M phase. Elutriation fraction 10: disrupted nuclear membrane with large holes (A)–(D). Elutriation fraction 12: linear arrangement of condensing chromosomes (A)–(C), sticky precondensed chromosomes (D). Bars 5  $\mu\text{m}$  each

the replicative DNA synthesis peaks in CHO cells. Nuclear growth takes place in several subphases [16] which are likely to correspond to the number of subphases of chromosome replication and to the number of chromosomes [24]. Further coincidence, namely the binding of cadmium to membrane proteins and the fact that nuclear membranes could not be permeabilized after cadmium treatment also favor the idea that cadmium concentration could be lowered by its adsorption to membrane structures including the nuclear envelope. An explanation why cadmium treatment prevented the opening of the nuclear membrane could be that by damaging the cell membrane, cadmium increases the permeability of the cells interfering with reversible permeabilization and causing stickiness of the nuclear material obscuring chromatin structures.

It has been shown by others that lower and higher cadmium concentrations have different cellular effects [10, 14, 15]. These contradictory results can be explained by cadmium binding, lowering the inhibitory metal ion concentration to the subtoxic level which may then have an opposite stimulatory effect. Experiments are in progress to determine the cadmium binding capacity of cells by atomic absorption spectrometry (Banfalvi et al. unpublished results).



Genotoxicity on metaphase chromosomes in mammalian cells *in vitro* were found only at highly cytotoxic concentrations of cadmium. Reduced metaphase number and shortening of metaphase chromosomes were detected in McCoy fibroblast cells exposed to 100  $\mu\text{M}$   $\text{CdSO}_4$ . The cell nucleus was labeled within one hour exposure to  $^{109}\text{Cd}$ , which suggested an early nuclear involvement in Cd-induced cell damage [25]. Two modes of action are likely to be predominant: the induction of oxidative DNA damage, best established and the interaction with DNA repair processes, leading to enhanced genotoxicity [22, 26].

However, these changes do not exclude interphase chromatin damages taking place before chromosome condensation. In fact characteristic nuclear changes induced by cadmium included apoptotic bodies in early S phase, smaller holes in mid S phase and larger holes and disruption in the nuclear membrane in late S phase. Such toxic chromatin changes were visible throughout the cell cycle in CHO cells [16]. We regard the holes and disruptions in nuclei as diagnostic symptoms of cadmium toxicity. These chromatin changes seem to be adequate endpoints for genotoxic effect-biomonitoring in cadmium exposed cells and organisms.

Regarding the questions addressed in the introduction it is logical to assume that: 1. There is no direct relationship between cell size and cadmium toxicity since the shrinkage of small cells in early S and large cells in late S, G2 and M phases is distinct from those in mid S phase. The density of the cell culture influences cadmium toxicity, high cell culture density reduces cytotoxicity probably by binding and lowering metal ion concentration. 2. The contradiction between the lower stimulatory Cd concentrations on DNA synthesis versus inhibitory effect of higher Cd concentrations could be explained by the shift from replicative to repair DNA synthesis. At low Cd concentration (0.2–5  $\mu\text{M}$ ) the replicative DNA synthesis is gradually inhibited, but this inhibition is less than the increase in repair DNA synthesis and the overall rate of DNA synthesis will be higher than in normal untreated cells. Several studies have shown that Cd interferes with DNA repair. Exceeding the tolerable level of Cd concentration repair synthesis is unable to cope with DNA damages. Consequently high Cd concentrations will inhibit both replicative and repair synthesis and cells undergo apoptosis. 3. The increase in cellular and nuclear size at lower concentrations of Cd is likely to be the reflection of an increased metabolic load manifested in the induction of both cytoplasmic and nuclear processes to overcome the toxic effect. Apoptotic levels of Cd toxicity result in the complete breakdown of metabolic activity seen as cellular and nuclear shrinkage.

**Acknowledgments** This work was supported by the OTKA grant T042762 (G.B.). This research was supported in part by the VA Merit Review grant and the DK58324-01A1 grant from the National Institutes of Health (A.G.B.).

## References

1. International Agency for Research on Cancer, Beryllium, cadmium, mercury and exposures in the glass manufacturing industry (1993) International Agency for Research on Cancer Monographs on the Evaluation of Carcinogenic Risks to Humans. Lion: IARC Scientific Publications 5:119–237
2. Jin T, Lu J, Nordberg M (1998) Toxicokinetics and biochemistry of cadmium with special emphasis on the role of metallothionein. *Neurotoxicology* 19:529–535
3. Bertin G, Averbeck D (2006) Cadmium: cellular effects, modifications of biomolecules, modulation of DNA repair and genotoxic consequences (a review). *Biochimie* 88:1549–1559
4. Dong S, Shen HM, Ong CN (2001) Cadmium-induced apoptosis and phenotypic changes in mouse thymocytes. *Mol Cell Biochem* 222:11–20
5. Fang MZ, Mar W, Cho MH (2002) Cadmium affects genes involved in growth regulation during two-stage transformation of Balb/3T3 cells. *Toxicology* 177:253–265
6. Waisberg M, Joseph P, Hale B, Beyersmann D (2003) Molecular and cellular mechanisms of cadmium carcinogenesis. *Toxicology* 192:95–117
7. Yang PM, Chiu SJ, Lin KA, Lin LY (2004) Effect of cadmium on cell cycle progression in Chinese hamster ovary cells. *Chem Biol Interact* 149:125–136
8. Oh SH, Lim SC (2006) A rapid and transient ROS generation by cadmium triggers apoptosis via caspase-dependent pathway in HepG2 cells and this is inhibited through N-acetylcysteine-mediated catalase upregulation. *Toxicol Appl Pharmacol* 212:212–223
9. Hamada T, Tanimoto A, Sasaguri Y (1997) Apoptosis induced by cadmium. *Apoptosis* 2:359–367
10. Hart BA, Lee CH, Shukla GS, Shukla A, Osier M, Eneman JD, Chiu JF (1999) Characterization of cadmium-induced apoptosis in rat lung epithelial cells: Evidence for the participation of oxidant stress. *Toxicology* 133:43–58
11. Watjen W, Cox M, Biagioli M, Beyersmann D (2002) Cadmium-induced apoptosis in C6 glioma cells: mediation by caspase 9-activation. *Biometals* 15:15–25
12. Rouzaire-Dubois B, Malo M, Milandri JB, Dubois JM (2004) Cell size-proliferation relationship in rat glioma cells. *Glia* 45:249–257
13. Kreuzer M, Kreienbrock L, Muller KM, Gerken M, Wichmann E (1999) Histologic types of lung carcinoma and age at onset. *Cancer (Phila.)* 85:1958–1965
14. Misra UK, Gawdi G, Pizzo SV (2003) Induction of mitogenic signalling in the 1LN prostate cell line on exposure to submicromolar concentrations of cadmium. *Cell Signal* 15: 1059–1070
15. Von Zglinicki T, Edwall C, Ostlund E, Lind B, Nordberg M, Ringertz NR, Wroblewski J (1992) Very low cadmium concentrations stimulate DNA synthesis and cell growth. *J Cell Sci* 103:1073–1081
16. Banfalvi G, Gacsi M, Nagy G, Kiss ZB, Basnakian AG (2005) Cadmium induced apoptotic changes in chromatin structure and subphases of nuclear growth during the cell cycle in CHO cells. *Apoptosis* 10:631–642
17. Offer H, Zurer I, Banfalvi G, Rehak M, Falcovitz A, Milyavsky M, Goldfinger N, Rotter V (2001) p53 modulates base excision activity in a cell cycle-specific manner after genotoxic stress. *Cancer Res* 61:88–96
18. Basnakian A, Banfalvi G, Sarkar N (1989) Contribution of DNA polymerase delta to DNA replication in permeable CHO cells synchronized in S phase. *Nucleic Acids Res* 17:4757–4767
19. Banfalvi G, Sooki-Toth A, Sarkar N, Csuzi S, Antoni F (1984) Nascent DNA synthesized reversibly permeable cells of mouse thymocytes. *Eur J Biochem* 139:553–559

20. Banfalvi G, Poirier L, Mikhailova M, Chou MW (1997) Relationship of repair and replicative DNA synthesis to cell cycle in Chinese hamster ovary (CHO-K1) cells. *DNA Cell Biol* 16:1155–1160
21. Nordberg GF, Jin T, Nordberg M (1994) Subcellular targets of cadmium nephrotoxicity: Cadmium binding to renal membrane proteins in animals with or without protective metallothionein synthesis. *Environ Health Perspect* 102:191–194
22. Banfalvi G, Littlefield N, Hass B, Mikhailova M, Csuka I, Szepessy E, Chou MW (2000) Effect of cadmium on the relationship between replicative and repair DNA synthesis in synchronized CHO cells. *Eur J Biochem* 267:6580–6585
23. Nagy G, Gacsi M, Rehak M, Basnakian AB, Klaisz M, Banfalvi G (2004) Gamma irradiation-induced apoptosis in murin epre-B Cells prevents the condensation of fibrillar chromatin in early S phase. *Apoptosis* 9:765–776
24. Banfalvi G, Mikhailova M, Poirier LA, Chou MW (1997) Multiple subphases of DNA replication in CHO cells. *DNA Cell Biol* 16:1493–1498
25. Fighetti MA, Miele M, Montella A, Desole MS, Congiu AM, Anania V (1988) Possible involvement of nuclei in cadmium-induced modifications of cultured cells. *Arch Toxicol* 62:476–478
26. Hartwig A (1995) Current aspects in metal genotoxicity. *Biometals* 8:3–11